agronomy

MDPI

Article

System Design and Validation of a Wireless Sensor Monitoring System in Silage

Josef J. Bauerdick [1,*], Hubert Spiekers [2] and Heinz Bernhardt [1]

[1] Chair of Agricultural Systems Engineering, Department of Life Science Engineering, TUM School of Life Sciences, Technical University of Munich (TUM), Duernast 10, 85354 Freising, Germany; heinz.bernhardt@tum.de

[2] Institute for Animal Nutrition and Feed Management, Bavarian State Research Centre for Agriculture (LfL), Prof.-Duerrwaechter-Platz 3, 85586 Poing-Grub, Germany; hubert.spiekers@lfl.bayern.de

* Correspondence: josef.bauerdick@tum.de

Abstract: Silages have become the main feed for ruminants and biogas production and are often stored in large stacks. When a silo is filled, a plastic cover is laid out and fermentation begins. From this moment, the entire silo becomes a black box for farmers: if any spoilage due to air breaches takes place, it often will only be recognized when the stack is opened and massive losses have already occurred. In the present work, a wireless sensor monitoring system for silage stacks is designed that shall detect changes in the silage environment until feedout and can therefore enable the farmer to prevent biomass losses. The nail-shaped node design offers elevated feed safety opportunities and can be easily removed before feedout. For data transmission, LoRaWAN is used in combination with a hardware-based timer. The sensor nodes are able to endure the full extent of a silage stack storage period in a full-scale silage test of approximately 40 weeks without battery shortage. The resulting measurements show that CO_2, O_2, relative humidity and temperature sensors at the silage surface can detect changes within the silage environment due to air breach. Temperatures in stable regions beneath 40 cm can be detected and give information about long-term stability.

Keywords: silage sensor; wireless sensor system; silage monitoring; air breach detection; silo controlling

Citation: Bauerdick, J.J.; Spiekers, H.; Bernhardt, H. System Design and Validation of a Wireless Sensor Monitoring System in Silage. *Agronomy* **2022**, *12*, 892. https://doi.org/10.3390/agronomy12040892

Academic Editor: Dionisio Andújar

Received: 16 March 2022
Accepted: 4 April 2022
Published: 7 April 2022

1. Introduction

Silage quality is of paramount importance with respect to ruminant feeding and in biogas production operations [1–4]. More than ever, the decline in cow grazing in Europe [5] stipulates the need for premium forages to ensure optimal productivity. To guarantee a high-quality silage, establishing an airtight seal directly after ensiling is necessary, which can be achieved by covering the ensiled material with plastic [6]. Without a seal, silage quality is impaired due to energy and dry matter losses [7]. When the plastic film is damaged, air ingress occurs; when combined with bad compaction rates, yeasts and molds multiply, inducing massive losses inside the silage [8].

According to Köhler et al. [9], losses inside the silage stack in particular must be reduced. To maintain an elevated level of silage quality, consistently executed controlling of the silo is recommended. Although it is possible to conduct silage controlling, as mentioned by several authors [10–12], this is often only performed selectively. Consequently, once the silage stack is sealed, the whole silo becomes a "black box" for farmers. For the reasons mentioned, the automated controlling of silages could potentially assure higher quality [13] and prevent losses, thereby greatly benefiting farmers with regard to economical savings. Furthermore, if losses are minimized, the carbon footprint of fodder-making could be as well [14]. To date, however, no automated systems for detecting destructive conditions in silage have been put into practice, despite extensive research on this topic since the 1990s, exhibited by [15].

Initial attempts of sensor-based silage controlling tools were invasive to the plastic cover, leading to breakage of the airtight film [16]. However, such invasive approaches are not expedient. Any detectable breach of the film must be methodically sealed to prevent a point of entry for oxygen or rainwater itself [15]. Yet, few investigations of noninvasive methods of silage controlling based on the wireless sensor networks have been published. For the first time, such an approach for practical use in agriculture was reported by [15]. The authors collected temperature and humidity data within the silage, as well as air and soil temperature outside of the silage stack. An improved approach of this research was shown by [17], now additionally equipped with an oxygen sensor. Another attempt was shown by [18], based on temperature and pH value. Despite [17] concluding with the perspective that their diagnostic system can be implemented in a farm management information system (FMIS), no implementation has so far taken place. Nonetheless, an automated sensor-based system for monitoring potential threats in the silage environment would be a powerful tool to maintain silage quality.

In this paper, we show a novel system design for a silage monitoring system based on a wireless sensor network that can detect silage environment deviations caused not only by air breaches, attained by collecting additional factors rather than exclusively temperature or oxygen. Conducive to reaching a high level of practicability, emphasis is placed on simplicity, reliability, and applicability. Furthermore, the system shall be tested under practical conditions, not only to record normal silage behavior, but to also capture air breach events and reach a Technology Readiness Level 5.

For the system design, several aspects must be considered:

- Hardware development (node);
- Connectivity;
- Energy management;
- Data management.

For testing the system, a threefold approach is chosen:

- Pre-testing (sensor validation) in jars (year 1);
- Testing prototype in field conditions (year 1);
- Field testing on TUM research farm (year 2).

Supplementary to capturing datasets pertaining to the statistical analysis of sensor system performance and silage stock processes, field testing provides insights into the practical handling and limitations of the sensor system regarding insertion, exertion, maintenance, and general handling.

Within the iterative development process, two distinctive sensor iterations have been developed and proofed.

Following a review of the present literature, this article shows three different parts of the system development. In each main chapter, the basic module design requirements are first addressed (Sections 3.1, 4.1 and 5.1), followed by hardware and connectivity specifications (Sections 3.2, 4.2 and 5.2) and finally testing and validation (Sections 3.3, 4.3 and 5.3), before imparting a final conclusion.

2. Literature Review

2.1. Silage Process

The basic principles of ensiling must be accounted for in order to set measurable parameters. Immediately after airtight sealing of green material, ensiling begins. This is driven by anaerobic fermentation of the fodder, established by lactic acid bacteria [19]. Ensiling and storage can be divided into different stages. These include the "aerobic phase", "fermentation phase" and "stable phase". A fourth phase following storage is designated as the "feed-out phase" [19,20]. When silage is sealed airtight, the remaining oxygen is discharged [19]. H_2O, CO_2 and NH_3 are formed from water-soluble carbohydrates and proteins [20]. These conversion processes lead to an increase in silage temperature. One defining characteristic of the aerobic phase is the brief duration, which lasts only a few

hours [10,19,21]. The subsequent silage fermentation phase then begins with a distinct shift to an anaerobic status. A rapid emergence of lactic acid bacteria further favors fermentation, leading to a pH value decrease [19,20,22]. However, anaerobic germs are still able to multiply, which can lead to spoilage [21,23]. Typically, within this phase, nitrous gases such as N_2O, NO and NO_2 [24] as well as NH_3 are formed [25,26]. If sealing coverage is sufficient, this gas formation can be seen at the very beginning of the fermentation phase by a rising of the plastic film [27]. Combined with moisture, some of these gases react, yielding aggressively dangerous nitrous acids [21,27]. When the fermentation process ends, nitrous gas concentrations decrease as they are reduced to N_2 und H_2O [24].

During the aerobic and fermentation phases, the levels of CO_2 and N_2 rise to a sum of nearly 100% of the total gas concentration beneath the film [28]. According to Wang and Burris [24], nitrogen is displaced by carbon dioxide throughout this step. However, no specific ratio between N_2 and CO_2 is given. Most of these changes occurring within the silage will endure the storage period. Respectively, the silage is in a stable phase and only few proteins and sugars are dismantled [19,21].

The literature indicates that gas flow inside silage is limited [15,29]. It can therefore be deduced that sufficient gas measurements must take place close to the silo surface. If the film is damaged, air will enter the area beneath the film, resulting in a change in the silage atmosphere prior to silage spoilage. Likewise, temperatures at the surface thereafter will also change due to spoilage. Within the silage stack, however, temperatures should be stable below 40 cm and not influenced by external temperatures [30]. Consequently, silage temperatures within the stack and at the surface may be important variables for long-term stability measurements.

2.2. Wireless Sensor Networks in Agriculture

According to [31], despite agriculture being one of the foundational systems of our world, it has not yet been thoroughly digitalized. The authors attribute this to the multifactorial, complex production system. Nevertheless, due to cost effectiveness, low power consumption, and easy implementation, wireless sensor networks (WSNs) have been receiving more attention in present day (precision) agriculture [31–33], horticulture [34,35] and smart cities [36]. As one of the most important aspects of the Internet of Things (IoT), sensor nodes within a WSN are capable of sending data from areas that are hard to access or within hostile environments [36]. Often, the data within agricultural WSNs can be considered modest in size [32], so that even low-power wide-area networks (LPWANs) can be used. For applications requiring wireless data transmission, a variety of wireless communication technologies are given in [37,38]. Their advantages and disadvantages are shown by [38]. The implementation of WSNs and different topologies, protocols and architectures are given as shown by [36]. The properties of a WSN are dependent on the amount of data to be sent and energy consumption and supply, but also shielding of the wireless signal. Especially prevalent in the agricultural context is the lack of grid-supplied power due to rural distances, making batteries, solar panels, and low-power soft- and hardware designs a necessity [32]. Actual research often shows a setup for WSN up to simulations or the visualization of gained data [36,37,39,40] and includes the stages "(i) data collection, (ii) processing, (iii) data analysis, and (iv) decision making" [34]. The rapid evolution of such WSNs shows the need for data protection against third parties within the whole network system, "from the source node (origin) to the receiver (destination) in the communication network and application for data processing and storing" [31].

2.3. Technical Fundamentals of Existing Silage Monitoring Tools

Only two attempts have been made to implement a noninvasive sensor node for silage. The technical parameters of these attempts are described below.

In the first-ever mentioned attempt, described by [15,17], data transmission took place wirelessly via a 433 MHz transceiver and a 10-bit A/D converter within a single hop network system. A single 3.6 V, 1.2 Ah lithium battery acted as the power source [17].

Battery life was estimated to be 120 days. The sensor nodes were ball-shaped and meant to be implemented between 50 to 10 cm beneath the silage surface [15,17]. The material used for the protective housing was not mentioned. Next to temperature, humidity and later oxygen, weather data were obtained to feed a computational fluid dynamics (CFD) model to predict temperature and oxygen trends of the silage. Tests were only conducted in a test silo of 3 × 1.5 × 0.5 m (lwh), not under direct practical conditions. The results were not sufficient as the model showed deviations between prediction and actual oxygen and temperature levels, directly after the beginning of the trial [17]. The actual behavior of the sensors when an air breach is conducted therefore cannot securely be described.

Thünen et al. [18] utilized temperature and pH sensor technologies to predict silage spoilage. Additionally, movement and position were gained to retrieve the sensor node within the silage stack during the feed-out phase. A density sensor was intended to give feedback about the silage density during the ensiling phase. The temperature sensor in this case had a range of −20–100 °C with an accuracy of 0.5 °C. Two 3.6 V, 13 Ah LSH20 Lithium batteries provided a power source. The estimated battery time was one year. Data transmission in this research was achieved by using a 169 MHz Band. Communication between the nodes and Gateway worked bidirectionally. This node resembles the node by [15,17] but is additionally equipped with a spike in which the pH sensor takes place. The node is made of Acrylonitrile Butadiene Styrene (ABS) using a 3D printing process. Since this node also serves as a density sensor for the silage, it must be placed during ensiling and is therefore also located inside the silage, underneath the surface. Tests in large-scale silage stacks were primarily conducted, e.g., to confirm general measurement and data transmission possibilities and the general functionality. Furthermore, in this study, no test was described assessing air infiltration under practical conditions.

The above-mentioned research presented limits regarding implementation, usability, and results. At no point were air breaches under practical conditions in a large-scale silo evaluated and until presently, the sensors have not been factored into practice. The behavior of those systems under legitimate practical conditions in addition to a conducted air breach cannot be described as sufficient.

3. Materials and Methods

The scheme of the Technology Readiness Level (TRL) is followed in this research paper. According to [41], the TRLs "are used to assess the maturity of a new technology towards full economic operation." The TRL scale consists of 9 steps, from TRL 1 to TRL 9 which are, e.g., defined by DIN-EN 16603-11 [42], or by [43]. By the end of this chapter, TRL 1 (basic principles observed and reported) and TRL 2 (technology concept and/or application formulated) will be reached. Over the course of the experiment, Technology Readiness Level (TRL) 5 (component critical function verification in a relevant environment) and the beginning of TRL 6 (model demonstrating the critical functions of the element in a relevant environment) [42] shall be reached.

3.1. Module Design Requirements

Following Green et al. [15], a wireless sensor node inside a silage stack has several advantages. According to the authors, the cover is still sealed and a long-term data collection with suitable scales and resolutions (compared to traditional methods) is provided. Furthermore, they state that a "wireless sensor's intimate connection with its immediate physical environment allows each sensor to provide detailed information that is difficult to obtain through traditional instrumentation such as invasive electrodes or probes."

Sensor nodes must be able to withstand the detrimental environment of silage. The benefits of a housing structure include robustness against influences from silage, protection of sensors and other electronics, as well as protection of the silage against defective electronics; a possibility in such instances as leaking batteries. These properties are seen as the minimum requirements for a sensor node.

As the literature shows, changes are anticipated, especially at the silage surface. To locate the node securely and retrievably, its head should stay even with the silage surface and its body must contain all necessary sensors and hardware. Requirements of the system for practical usage include both easy insertion and easy removal of the sensor node.

Before any spoilage of the silage is visible, losses between 5–20% may already be present [44]. It can be conveyed, therefore, that changes within the silage and the silage atmosphere take place inertially. Consistent with these parameters, measurements in the silo stock with a time interval of up to one hour are sufficient to record changes. Between measurements, the sensors can be shut down to save battery.

3.2. Hardware and Connectivity Specification

To develop a comprehensive overview about the silage state, a variety of sensors are needed. After reviewing the silage-related literature, the following parameters shall be tested regarding their information value for the proposed aim:

- Temperature (°C) at surface and in 40 cm depth,
- Oxygen concentration (%),
- Carbon dioxide concentration (%),
- Humidity (%),
- Air pressure (hPa).

3.2.1. Sensors and Batteries

As the standard storage time of a silo can last up to one year, specific required sensors were chosen to account for low energy consumption to facilitate 365 days of measurement. Further technical requirements of all sensors are composed of adequate measurement ranges. With respect to temperature, values from −30 °C (depending on the local climate) up to 70 °C (representative of a hot summer day with high sun exposure) should be anticipated. Oxygen sensors maintaining a measurement range between 0 and 21% (actual amount in the air) are functionally sufficient. As the literature demonstrates, CO_2 and N_2 add up to an amount of 100% in total. As no specific maximum is shown in the literature, a CO_2 sensor with a range from 0 to 100% is assumed to be capable of measuring any amount present. Regarding humidity, it is known from the literature that water is a decomposition product consequent of ensiling. Therefore, a humidity sensor with a measurement range from 0 to 100% is obligatory. No specific information regarding air pressure is given in the literature. Thus, a standard air pressure sensor capable of collecting measurements between 15 to 115 kPa would be appropriate. To satisfy these requirements, a variety of off-the-shelf sensors could be used, especially for temperature, humidity, and air pressure measurements. However, to utilize oxygen and carbon dioxide sensors that meet the requirements, a limited number of sensors show adequate performance. For a better overview, the sensors are listed in Table 1. As two distinctive sensor iterations have been developed and proofed, both hardware properties are shown in the following.

As temperature sensors in early-stage nodes, the temperature modules "RTR-502L" by T&D corporation with a measuring range of −60 to 155 °C and an accuracy of ±0.3 °C at −20 to 80 °C were used. The second sensor generation was equipped with analogue Pt100 sensors of accuracy type B and a MU-PT100-U010 transducer to convert output voltage to a range from 0 to 5 V.

Table 1. Overview of used sensors and their power source in the present nodes. The correct voltages needed were provided by DC-DC converter.

	Used Sensors in This Research	
	RTR–Nodes Iteration 1	**LoRa–Nodes Iteration 2**
Temperature	RTR-502L by T&D corp. Range: −60 to 155 °C Accuracy: ±0.3 °C at 20 to 80 °C Power source: own battery	Pt100 by B + B Thermo Range: −40 to 180 °C Accuracy type B (±0.3 °C at 0 °C) Power source: 6 × 3.7 V, 4500 mAh
Oxygen	ME2-O2–Φ 20 by Zhengzhou Winsen Electronics Technology Co., Ltd. Range: 0 to 15% O_2 Sensitivity: 0.05~0.15 mA Power source: 4 × 1.2 V, 13,000 mAh NiMh	Power source: 2 × 1.2 V, 13,000 mAh NiMh
Carbon dioxide	COZIR Wide Range Sensor by gassensing.co.uk Range: 0–100% CO_2 Accuracy: ±5% CO_2 Power source: 4 × 1.2 V, 13,000 mAh NiMh	Power source: 2 × 1.2 V, 13,000 mAh NiMh
Humidity	HIH-4000 by Honeywell Range: 0–100% RH Accuracy: ±3.5% TH Power source: 2 × 3.7 V, 4500 mAh	Power source: 6 × 3.7 V, 4500 mAh
Air pressure	MPX4115 by Freescale Semiconductors Range: 15–115 kPa Accuracy: ±3.5% Power source: 2 × 3.7 V, 4500 mAh	Power source: 6 × 3.7 V, 4500 mAh

A chemical "ME2-O2-Φ 20 Oxygen Sensor" from "Zhengzhou Winsen Electronics Technology Co., Ltd." with a measuring range of 0 to 25% was used for the detection of O_2 with a sensitivity of 0.05~0.15 mA in the air and an input voltage of 3.3 or 5 V [45]. A pre-heat time period of about 30 min is required [45].

For CO_2 measurement, an NDIR-based "COZIR Wide Range Sensor" (0 to 100%) with an accuracy of ±5% and a 3.3 V current supply was chosen. Energy consumption is specified with 22 mA [46].

An HIH-4000 Sensor by Honeywell is powered for relative humidity measurement. Supply voltage amounts may range between 4 to 5.6 V with typical 200 µA and maximum 500 µA current supply. Accuracy is specified with ±3.5% [47].

For air pressure, an MPX4115 with a supply voltage of 4.85 to 5.1 V and 7 to 10 mA current supply is used. Accuracy is specified with ±1.5% [48].

For initial tests, 868 MHz data transmission modules are used. These modules, named "RTR-500", are provided by T&D Corporation, Matsumoto, Japan. Each RTR module has its own battery (Saft LS 26500) with 3.6 V and 7.700 mAh, which includes the temperature sensors. Within the RTR nodes, 4 NiMh batteries with 1.2 V and 13,000 mAh power oxygen and carbon dioxide sensors, which run at 3.3 V, and two Li-ion 26,650 with 3.7 V and 4500 mAh are used for powering air pressure and humidity sensors at 5 V. For a better overview, power sources are assigned to the individual sensors in Table 1.

In the second node iteration, LoRa transmission modules "Arduino MKR 1300" are used. LoRa is a wireless data transmission technology, which typically runs at 868 MHz in Germany [49]. Such boards consist of 8 digital I/O ports and 7 analog input ports. LoRa is

used as it is reportedly known for its wide range usage, relatively low power consumption and robustness against interferences [31,37]. Furthermore, the hardware is highly cost-efficient without monthly fees as required by the usage of other networks [37]. These nodes consist of one format of 6 Li-ion 26,650 with 3.7 V and 4500 mAh, each connected in series. These batteries power the microcontroller board, humidity and air pressure sensors with 5 V and two Pt100 sensors with 12 V. In another format, two 1.2 V and 13,000 mAh NiMh batteries empower oxygen and carbon dioxide sensors with 3.3 V (Table 1).

The introduced hardware must resist the oxidative environment within a silo. Basic hardware, such as transmitting modules, timer circuits or batteries can be secured by modification of node design within an extra housing. The sensors, however, must be exposed to the environment for adequate measurement collections. As no sensor fulfills any hardware protection requirements at factory default, the protection of used sensors must be ensured otherwise. For this purpose, an epoxy coating is tested.

3.2.2. Connectivity and Data Management

A wireless sensor node inside a silage stack on a farm requires a sufficient connectivity solution. Since silos can be built farther from the farm, reliable data transmission must be ensured even over distances greater than 100 m. Often on farms, no farm-wide area network is established. Therefore, a wireless data network with low power consumption and reliable data transmission needs to be installed from the node up to data storage and evaluation.

In the first sensor node iteration, to reach a high data resilience, each sensor is attached to an RTR module, which is capable of storing data for over seven days. Data packages of each sensor can be gained via an 868 MHz wireless connection on demand. If one RTR module fails, only the data of the sensor attached to this specific RTR module are lost.

Data from this first node iteration were manually collected via a gateway after ca. 7 days with the "RTR-500 for Windows" software and transformed into a .txt file. Manual transmission was chosen to ensure that no transmission issues lead to a lack of data.

The second sensor node iteration, equipped with a LoRa microcontroller, can obtain data from all sensors at the same time. As the network topology, a simple star topology is used, as only low influences by, e.g., obstacles, can be awaited, and a close line of sight can be assumed. Furthermore, due to the implementation of a hardware-based timer board, multi-hop systems are impractical. The LoRa microcontroller sends data automatically via 868 MHz when it awakens from deep sleep mode. Therefore, Over The Air Activation (OTAA) with an fixed authentication ("root") key within the LoRa device is used, which is recognized by the LoRaWAN network server for authentication. With the help of this authentication key, which will not be sent during a connection between device and gateway, so-called "session keys" are generated by the network server, which will be renewed by every new connection [50]. No data storage is given within this node. The data are sent to a Multitech MTCDT-246A-868-EU-GB LoRa gateway, which directs the data package via the Internet to a LoRaWAN Network Server, called "The Things Network". From this, the data are derived by a Raspberry Pi single-board computer and stored in a continuous .txt file for each node on Network-Attached Storage (NAS). The general structure of a wireless sensor network for such a purpose can be seen by [51] and is abstractly shown in Figure 1.

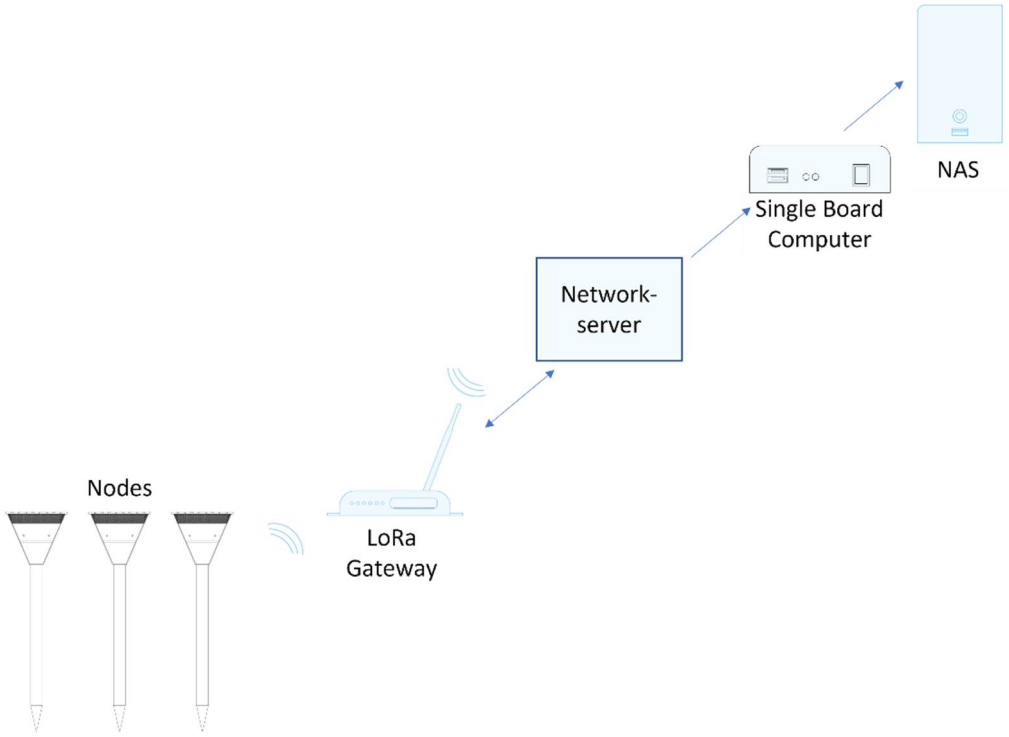

Figure 1. Structure of the LoRa wireless sensor network within this study. Data transfer from LoRa sensor nodes to LoRa Gateway happened wirelessly. The gateway as well as the single-board computer and the network-attached storage were connected via ethernet cable to the Internet.

Gateways for both sensor generations were placed inside a stable, at between 45 to 70 meters distance from sensor nodes. With self-programmed LabView programs, data packages were accumulated and then post-processed within R-studio.

3.3. Testing and Validation

Testing and validation is threefold in this research and will be conducted from a test under laboratory conditions to a small-scale test with the node design, concluding in a full-scale silage test.

3.3.1. Mason Jar Test

In order to reach TRL 3 (characteristic proof of concept) [42], a laboratory pretest of the designed sensors was conducted in a mason jar. Over a time span of 13 days, inside a 2-liter mason jar filled with unfrozen green grass material (200 g, 46% DM), oxygen, carbon dioxide, relative humidity and air pressure sensors were tested for general suitability. The material was not specifically compacted. Sensors were placed in the jar and connected via a cable to a computer running a LabView program. After insertion of the green grass material, the jar was sealed airtight to initiate the fermentation phase. A total of 221 h after closure of the jar, the lid was opened to simulate an air breach.

3.3.2. Test Silo

After the sensors demonstrated the capacity to detect changes under laboratory conditions in the mason jar, TRL 4 (component functional verification in laboratory environment) [42] was reached within this test. A test silo of 64 cm in diameter and with a height of 94.5 cm was filled and compacted with 206 kg of previously fermented grass silage (36.7% DM content, reconsolidated in 20 cm layers with 95 kg force per ~346 cm^2) from winter 2018 for 57 days (19 February 2018–16 April 2018). A conceptualized sensor housing with default data transmission modules was brought into the test silo, with all six sensors

attached, and the silo was sealed. After 35 days, a massive air breach was conducted, and the seal was broken with 4 holes of approximately 14 cm in diameter.

3.3.3. Full Scale Test

In order to reach TRL 5 (component critical function verification in a relevant environment) [42], the two different node configurations were tested in a full-scale silage stack experiment (config one 4 times, config two 7 times) at the Veitshof farm of the Technical University of Munich. Tests were conducted in grass silage from May 2019 till April 2020. The dry matter content was 50.3%, and the silo was compacted with a 16-ton wheeled loader with attached tires sized 20.5 R25 with 3 crossings per layer (max 30 cm per layer). The sensor nodes were brought into the silage after compaction and before the plastic film was laid out (Figure 2). After the storage phase, air breaches were conducted at two sites within a test field, equipped with seven nodes (A + B in Figure 2). Air breaches 1–3 and 5 took place at site A, air breach 4 at site B. Additionally, a weather station by "Lambrecht meteo" was installed at the silo site with the purpose of collecting temperature, global radiation, relative humidity and precipitation levels.

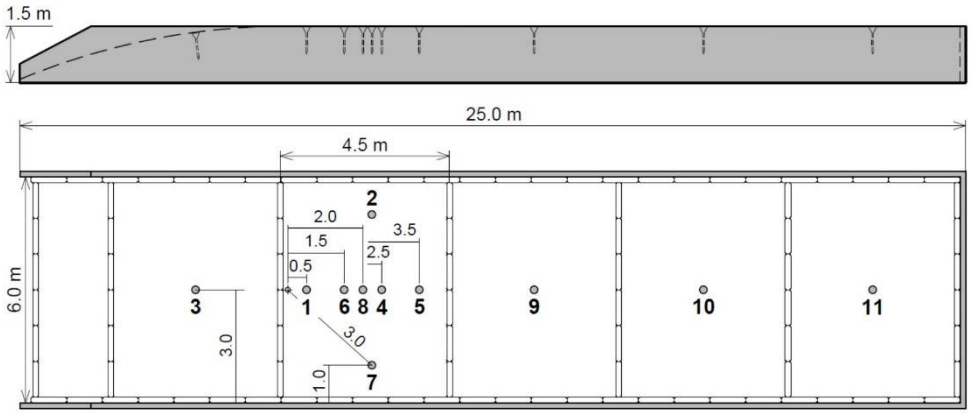

Figure 2. Test setup in large-scale silo. Numbers show the sensor nodes, (1–4 = iteration 1, 4–11 = iteration 2). Letters show two different sites of implemented air breaches.

4. Results

4.1. Module Design

Based on the literature review, a first house conceptualization was designed, which is shown in Figure 3. The sensor node consists of two separated containers and a spike. Within the inner container, data transmission modules as well as a hardware-based timer board and batteries were installed. This container is sealed airtight to protect the hardware from harmful outside influences in the environment. The second container ("Sensorvolume" in Figure 3) contains the oxygen, carbon dioxide and relative humidity sensors and is open against the silage environment via a tube of 5 mm diameter. As the pretests show elevated humidity, another tube located at the bottom allows the condensate to run out. Temperature was measured at two sites. The node head was equipped with one sensor to detect changes at the surface. The core temperature of the silage also gives information about long term stability; therefore, another temperature sensor was attached at the spike of the sensor housing. When LoRa Boards for data transmission were implemented, the node design was revised. A revised version is shown in Figure 4. The second-generation nodes (iteration two) have a smaller head as the spike now contains the batteries, and the LoRa microcontroller is smaller than the previously used RTR transmission modules. Accordingly, the spike's diameter is bigger in iteration two to contain the batteries (I1 = 25 mm, I2 = 34 mm). This resulted in issues implementing the sensor nodes into the silo.

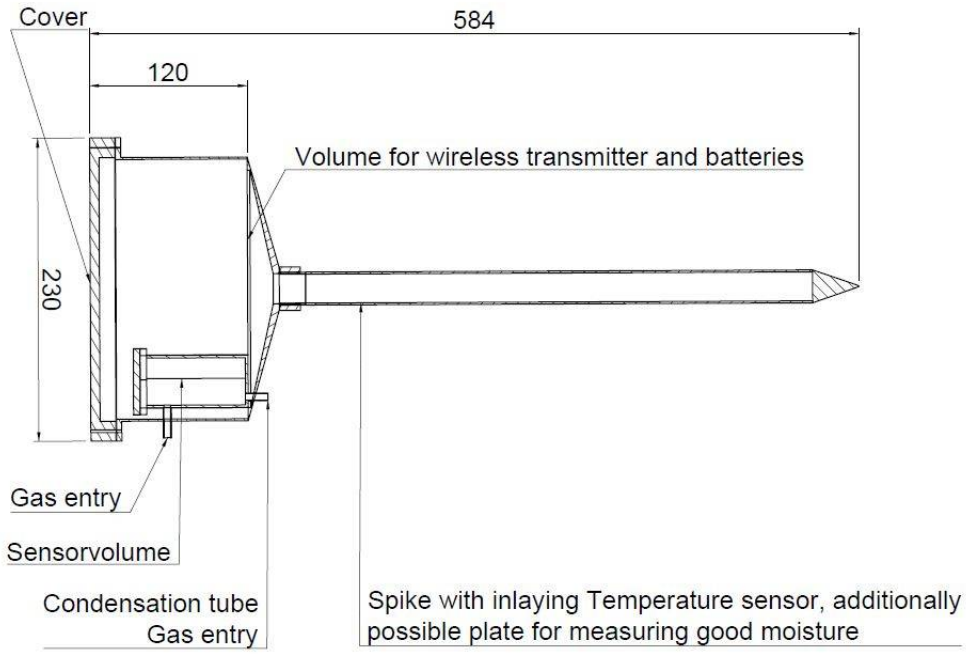

Figure 3. Schematic of the first-generation sensor node (drawn with Autodesk Fusion). After the initial small-scale silage test, a circumferential grill was applied and the gas entry was enlarged. Sizes are shown in mm.

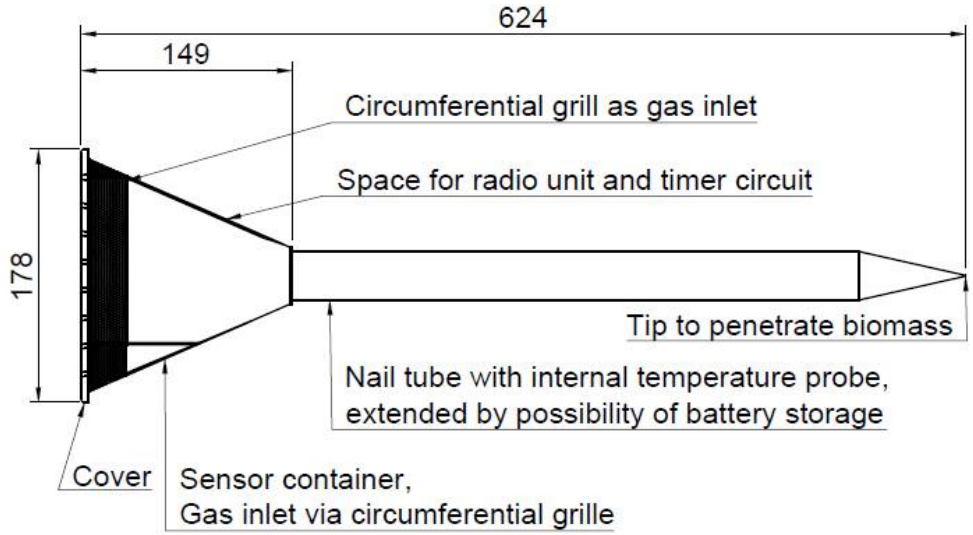

Figure 4. Schematic of the second-generation sensor node (drawn with Autodesk Fusion). The head is designed smaller, sensors come closer to the surface and an additional circumferential grill is applied to let gas enter the sensor container from all sides. The battery can now be positioned into the nail. Sizes are shown in mm.

4.2. Hardware and Connectivity Development Results

This section is divided into sub sections containing sensor durability, timer circuit and energy sufficiency, and connectivity of the nodes.

4.2.1. Sensor Durability

Results show that the silage environment is especially hostile to sensor systems. CO_2 sensors in particular exhibited damages due to oxidation within pretests. Functionality could be protected with a layer of epoxy resin. All sensors were coated with epoxy so that humidity and silage gases were not able to reach the electrical components (apart from

the actual sensor element). Even electrical joints that are located within the sensor were covered with epoxy resin to keep full functionality. However, after extraction, O_2 sensors indicated a lack of functionality in some cases, while RH sensors still worked sufficiently. As the temperature sensors are placed inside the hermetic hardware volume, these were not affected by the silage environment at all.

4.2.2. Timer Circuit and Energy Sufficiency

As mentioned in the aim of this work, the battery life of the sensor must endure at least a 365-day storage period. To ensure this aim, a hardware-based timer circuit was designed, based on an NE555 and two AQZ 202 PhotoMos to create an astable flip-flop. As the O_2 sensor requires a 30 min preheat time, it was not shut down by the timer circuit. Due to the implemented timer circuit, approximately every 17:03 min (ranging from 16:32 to 17:55 min), sensors are started, and one data package is delivered per node. Due to hardware specifications, which can differ within a part, and time of connection to the gateway, the mean time differed slightly between the nodes. So, within a day, approximately 84.5 measurements per node are possible when batteries are fully loaded.

Sensor iterations in this research were tested to evaluate energy consumption. Hereby, both power circuits (NiMh and Li-Ion) were considered separately. The results were calculated for a whole year. Results can be seen in Table 2. The capacity for each power circuit (NiMh and Li-ion) is sufficient for 365 days. The additional batteries for empowering the RTR data loggers are not shown within the table.

Table 2. Calculated energy usage and available amount of energy for a 365-day period of used node iterations, divided by battery circuits.

Energy Consumption of Used Sensor Iterations, Divided by Power Circuits		
Iteration	**Battery Capacity Total Available and Needed for 365 Days**	
	NiMh (1.2 V, 13,000 mAh Each)	**Li-ion (3.7 V, 4500 mAh Each)**
RTR Module 4 NiMh, 2 Li-ion	Capacity total: 52,000 mAh	Capacity total: 9000 mAh
	Capacity need: 16,619 mAh	Capacity need: 7705 mAh
LoRa Module 2 NiMh 6 Li-ion (two each connected in series = 7.4 V packs)	Capacity total: 26,000 mAh	Capacity total: 13,500 mAh
	Capacity need: 8866 mAh	Capacity need: 8608 mAh

4.2.3. Connectivity

The connectivity was evaluated within the large-scale silage test, with four repetitions of iteration one and seven repetitions of iteration two executed.

Data transmission of iteration one with RTR 500 modules was adequate despite transmission problems occurring sometimes. The data sampling rate of the RTR 500 modules was one point per minute as no specific options could be chosen by default (e.g., only measurements when voltage of sensors is high). As only oxygen and temperature were powered full time, the data density of these sensors exceeded the data density of the others, which showed valid measurements when being turned on by the timer board (after approximately 17:03 min). Due to minute interval measurements, zeros occurred in the data of CO_2, humidity and air pressure, which had to be extracted by post-processing. Approximately every 7 days, the stored data packages were manually transmitted via wireless connection. Several times within the trial, however, some modules' data could not be gained by the installed gateway as no connection to the modules could be established. As a result, an individual used a second gateway attached to a laptop and moved near (<3 m) to the nodes to transmit data from this point. These issues were not observed with iteration two nodes.

Figure 5 shows the course of the delivered data packets of the LoRa sensor nodes within the trial. Data were sampled when the timer circuit turned on the power after approximately 17:03 min. The "Received Signal Strength Indicator" (RSSI) values of the LoRa nodes were pending between −80 and −100. Sensor nodes were extracted from the silo at the point of silage removal. The delivered data packets are given in percentages, as each node was evaluated for its own maximum daily transmitted data packets (based on individual hardware properties, see Section 4.2.2). The graph shows that during the time of 35 weeks (afterwards, only 2 nodes were still in the silo), the amount of delivered data is decreasing, with a pronounced slump in Week 20. In week 38, another breakage of transmissions can be observed. Module 8 and Module 10 failed within the first 10 weeks due to technical defects and did not send any packages following. Module 5 showed low battery in Week 15. It is remarkable that from inception, node 7 only sends slightly more than 50% of possible data packets. The other nodes show a transmission rate of about 76% up to 85% (approximately 2.8 data packets per hour) at the beginning. During the trial, these rates decrease, so that at the end of the 40-week trial, around 50% of possible data packets are delivered, equivalent to approximately 1.7 data packets per hour.

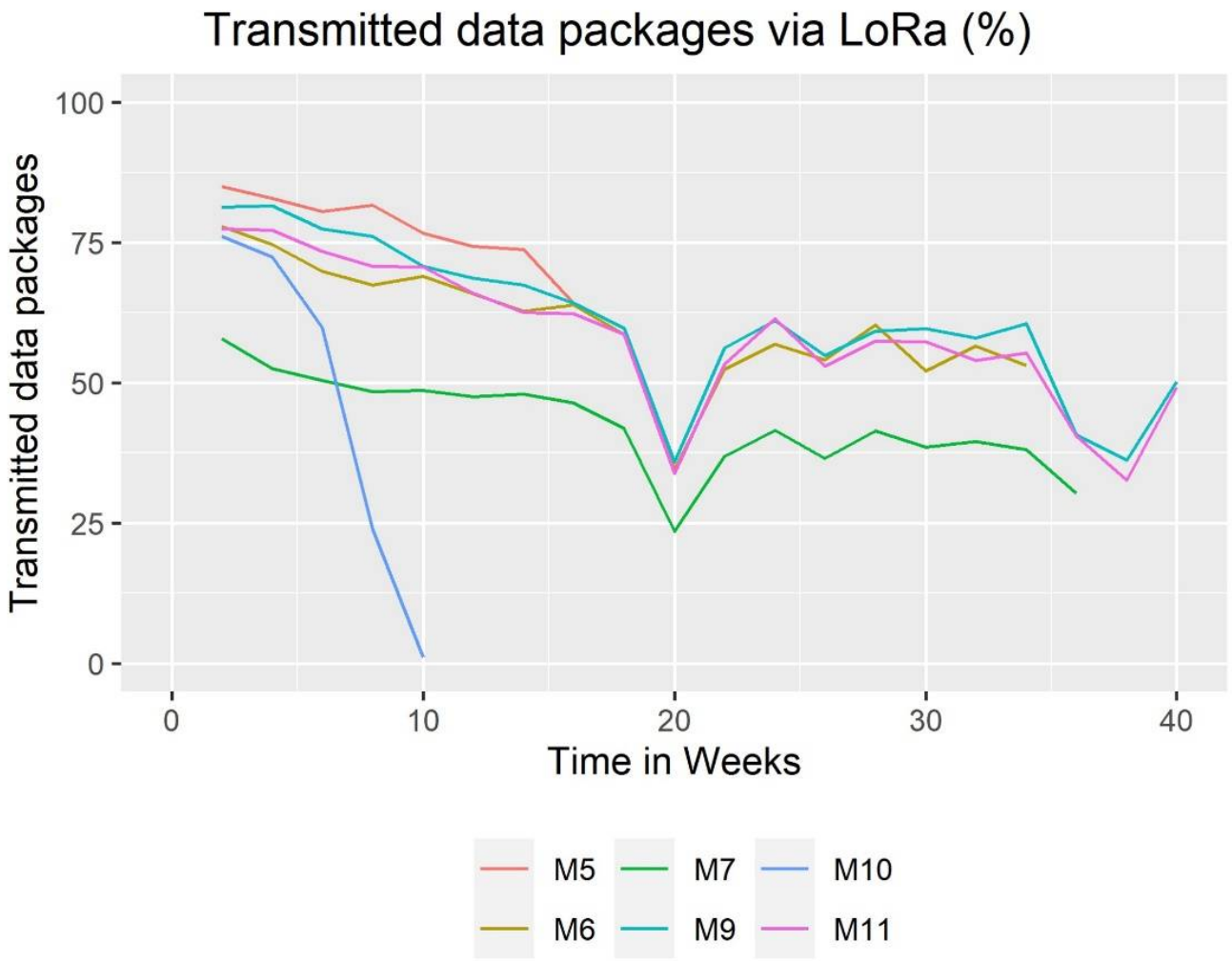

Figure 5. Data transmission rates in percent of LoRa nodes in trial 3 over a time span of 40 weeks. With the exception of M5 and M10, all nodes stop transmission when being extracted in feed-out phase. Battery of M5 was low by the 15th week of trial.

4.3. Testing Results

In the following section, the test results of the three scaled test are shown.

4.3.1. Mason Jar Test

The results of the laboratory test are shown in Figure 6. The oxygen curve decreased close to zero within 10 h, while CO_2 increased during the first 50 h before it reached a plateau. It is noticeable that within the test, O_2 showed an increase 23 h after the start, with a peak after 50 h before decreasing again. Humidity rose quickly within the first 25 h to more than 80% and continued rising afterwards. Air pressure is volatile and therefore showed no indication of being influenced by reactions within the jar. Overall, sensors have demonstrated that air ingress can be detected by proof of concept.

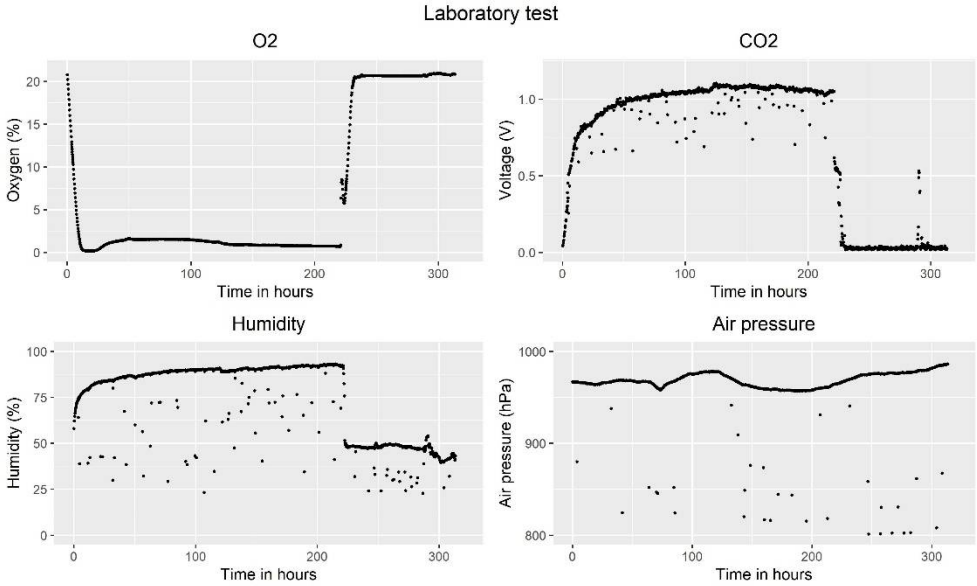

Figure 6. Laboratory test in a mason jar with green grass material. O_2 curve shows an increase after reaching zero already. CO_2 rises constantly, as well as humidity. Air pressure is not influenced by the ensiling process. When opening the jar after 221 h, O_2, CO_2 and humidity show clear breakdowns.

4.3.2. Test Silo

The results of the test silo test can be seen in Figure 7. Temperatures at the silage surface as well as in the spike show the same course. The only difference is that at the surface, a daily fluctuation can be seen. The temperatures were compared to measurements outside the trial and indicated that they imitate the outside climate. Similar patterns were observed with air pressure. O_2 decreases and CO_2 increases until the plastic cover was damaged after 840 h. These sensors demonstrated basic functionality. Humidity increased over the entire period; after opening the test silo, it could be determined that the whole silage surface had dried out down to 5 mm. Consequently, the module design was altered so that the surface of the sensor housing was enlarged and moved closer to the surface to detect any changes directly at the surface. The test silo proving scheme illustrates that these sensors, installed into the designed housing, fulfill basic requirements.

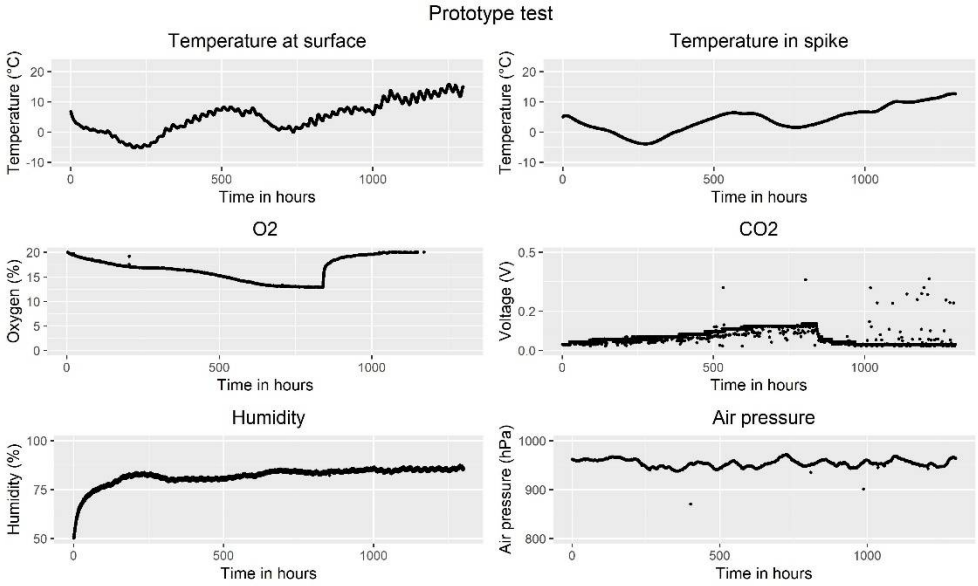

Figure 7. Results of the prototype test with already-fermented silage. Silage was extracted from a full-scale silo and re-ensiled in the test silo in winter. Temperatures at surface and in spike show the same patterns. At the surface daily variations are also seen. Oxygen decreases during the trial, while carbon dioxide rises. Both processes reverse as the test silo is opened. Humidity rises over the whole period, and air pressure shows no anomalies when compared with outside air pressure.

4.3.3. Full-Scale Test

Figures 8–11 show the air-breach section of temperature, CO_2 and O_2 from the large-scale silage test within the trial area of the silo. Temperatures at the surface are directly affected by outside temperatures. The core temperature underneath 40 cm shows a decreasing value over the 300-day period, with one exception from day 86 to day 93, where M4 increases from 28.7 °C to 32.1 °C and M6 from 29.3 °C to 30.1 °C. Some sensors show a slight increase shortly after an increase in outside temperature as well. During air breaches, temperature sensor values show no influence. As seen in the mason jar test, as within this test, the oxygen values decrease to 0 at the beginning of fermentation, before a clear ascent within a few days.

Within the conducted air breaches (grey highlighted), the O_2 sensors are capable of showing deviations from their normal behavior, especially at air breach B (#4, M2, M4, M6) and slightly during the last air breach (#5, M4, M6) at site A in which the breach was not cut but plucked to imitate a bird picking. The CO_2 levels show strong deviations of more than 5% (Figure 11). M1 and M6 in particular show breakages of more than 5% at each air breach. At air breach B, M4 also shows a breakage of values higher than 5%. However, not all sensors close to the air breach exhibited deviations. Sometimes sensors farther away from the breach showed such indications, while closer ones did not. Assessing Figure 11, CO_2 concentration within the silage rises to over 60% within a few hours. As observed, some sensors show a rise to only 40–50%. However, during the trial, the levels of carbon dioxide decreased.

Humidity sensors displayed only slight rises in value at certain breaches. However, these rises were less than 5%, and elevated daily amplitudes were observed during summer months (some sensors show amplitudes higher than 10%). As air pressure showed no differences to the outside pressure, it is not included in the results.

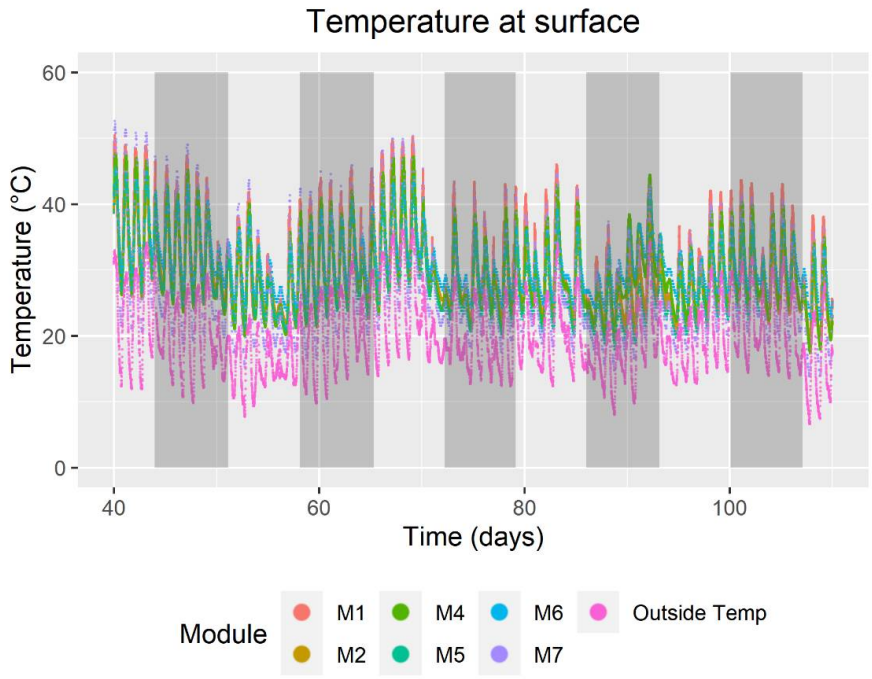

Figure 8. Temperature at surface during the full-scale test within the trial field. Grey highlighted are the conducted air breaches. Breaches 1–3 and 5 are at spot A, breach 4 is at spot B (Figure 2). It becomes obvious that outside temperature (pink) is always lower than surface temperature inside the silage. Nevertheless, the silage surface temperature shows a similar course to the outside temperature. As Module 8 broke within the first few days, it is not shown.

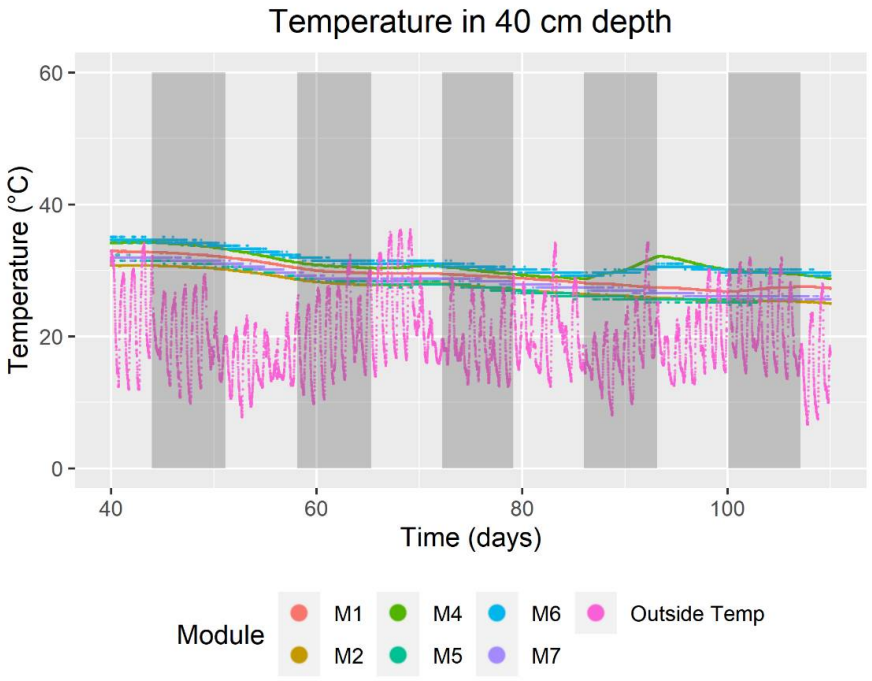

Figure 9. Temperature within 40 cm depth during the full-scale test within the trial field. Grey highlighted are the days of air breaches. Breaches 1–3 and 5 are at spot A, and breach 4 is at spot B (Figure 2). Over the whole storage period (300 days) the temperature decreased with a bigger exemption of Module M4 and M6 at days 86–93. Additionally, other modules showed slight increases in temperature when hot days preceded. As Module 8 broke within the first few days, it is not shown.

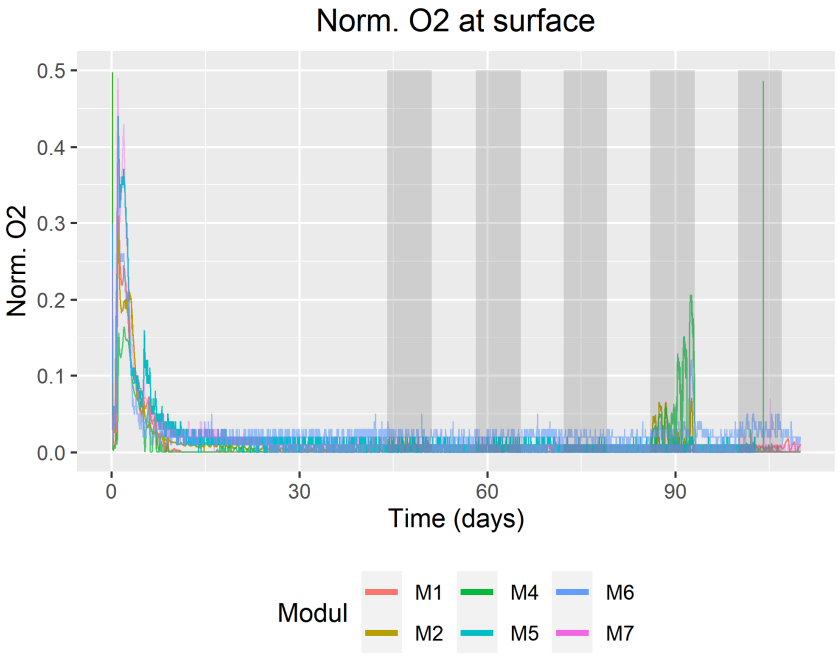

Figure 10. Normalized oxygen content during the full-scale test within the trial field. Grey highlighted are the days of air breaches. At the beginning of the trials, an unusual rise in the oxygen curve can be observed which can be traced back to a cross sensitivity to NOx gases. Breaches 1–3 and 5 are at spot A, and breach 4 is at spot B (Figure 2). During the air breaches, several sensors showed a rise in their curves and therefore indicate an air breach. When no abnormality is present, the values are pending close to zero. As Module 8 broke within the first few days, it is not shown.

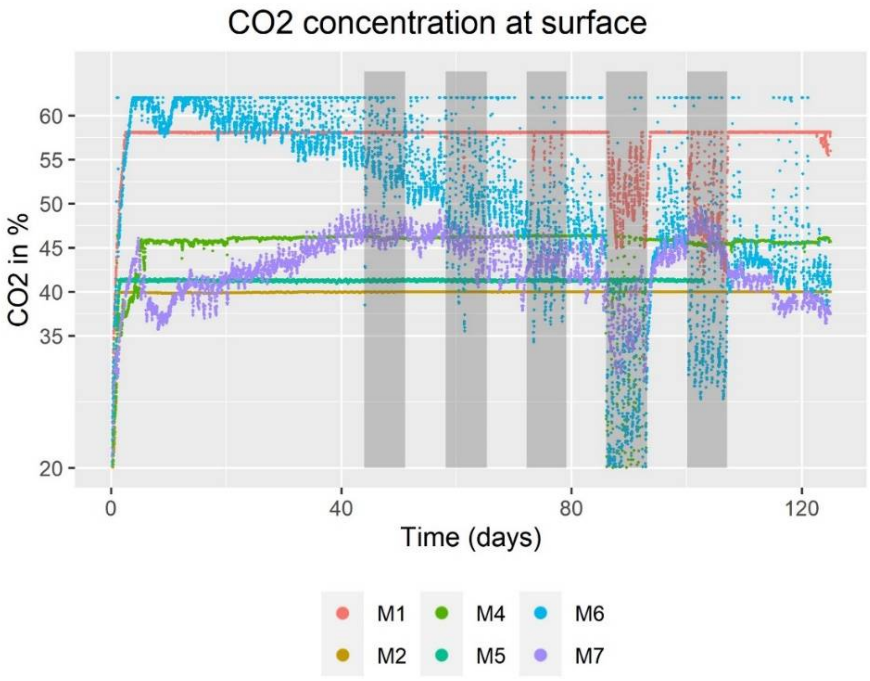

Figure 11. CO_2 concentration during the full-scale test within the trial field. As CO_2 sensors showed different calibrations, maximum amounts of CO_2 between each sensor differed. Within the grey highlighted areas, air breaches are conducted. Breaches 1–3 and 5 are at spot A, breach 4 is at spot B (Figure 2). As Module 8 broke within the first days, it is not shown.

5. Discussion

5.1. Module Design

The results largely show that it is possible to detect air breaches and spoilage within a silo with specifically designed sensor nodes. The design and insertion differ between previously reported research and the literature: it is not meant to be placed beneath the silage surface, but rather, the head should stay even with the silage surface and immersed into the silo after compaction, before putting the plastic on it. This way, gas sensors also stay at the surface and yield more reliable results than earlier published experimental attempts as gas flow within the silage is proven to be very limited [15,29]. The insertion method of the sensor was confirmed to be effective. In some cases, due to high compaction rates, it was necessary to predrill a hole for the spikes of the node with a steel stick. Removal from the other side was then feasible before feed-out so that no damage to the hardware was caused, a previously potential occurrence with silage removal machinery in research trials. As the node's heads were fastened with blue tape, their surface contrasted with the silage and were easily found. Due to the V2A steel, they could easily be pulled out. In general, applicability and handling of the sensor module appeared functional; high practicability is assumed. However, the module design should be developed in specific ways. One could improve the insertion of the modules further, by designing the nail as small as possible in diameter, while a thread on the nail could support insertion as well. As Rees et al. [29] state, silage typically has a low gas diffusion rate. Within the shown modules, all sensors except temperature are attached to one side of the module; they are connected to all sides with a grid and space for gas diffusion. While gas flow may find its way to the sensor devices, humidity in particular showed changes in the uppermost layer of silage within the test silo when air ingress occurred and should therefore be measured at the highest point possible. In a future generation, sensors should not be attached to a side of the module but on top of it, directly underneath a lid to be protected from direct heat from the sun. To reuse the node, even if a sensor is broken, sensors must be easily replaced, which can be also fulfilled by such a design. As the spike is open to the container, it satisfies a prerequisite for usage inside of the feed: in case a battery is leaking, undesirable contaminants will run and be stored inside the spike and not contaminate the fodder. Temperature measurements within 40 cm of depth can be seen as a good indicator to evaluate long-term stability of silage and therefore should be collected as well. Within this study, however, V2A steel was used as a basis for the sensor nodes. As metal has thermal conductivity, it is possible that outside temperatures can be forwarded down the sensor and influence the measurement, which was seen within the large-scale silage test. In node generation two, the batteries moved from the top of the node into the spike. In addition to the advantage that the head of the node becomes smaller, the batteries are now more insulated against strongly fluctuating temperatures in the node heads. The results of the tests show that temperatures in the region can exceed 50 °C in summer and dip lower than 0 °C in winter. With the obligatory sensors specified, an enhanced module can be created and plastic forming or 3D printing can be employed to create modules quickly and economically for future research.

5.2. Hardware Development and Sensor Protection

Bauerdick et al. [52] state that four distinct aspects cause sensor detriment on farms; these are humidity, coldness, heat, and corrosion. When placing a sensor inside a silage stack, all factors will influence the sensors. As can be inferred from the results, humidity increases to significant levels within a short amount of time when silage is sealed. Due to the fermentation, nitrous gases are formed, such as N_2O, NO or NO_2 [53]. Occasionally, these gases leak from the silo and can be identified as rust-brown fogs around the silo. When these gases react with humidity, nitrous acids can be formed which are extremely dangerous for humans [27]. These acids can also act as strong oxidizing agents [54] and therefore harm sensors and Printed Circuit Boards (PCBs) as well. Adapted sensor protection is therefore critical. The results show that an epoxy coating of the electronical parts of a sensor (limiting environmental exposure exclusively to the sensor element of the apparatus) is sufficient to

protect sensors against environmental hazards for an entire storage season. Oxygen level detection was established with chemical sensors in this trial. Since it cannot be ruled out that silage gases influence the chemical components of used sensors, in future research, chemical sensors should be replaced. Limited sensor lifetimes estimated by manufacturers must also be taken into consideration for all sensors in future research.

In the present research, a hardware-based timer was chosen. Software failure due to data storage issues or otherwise can therefore be avoided.

5.2.1. Energy Efficiency

Table 2 shows the available energy within the used sensor nodes, as well as the theoretical energy values required for a one-year storage period. The calculated results emphasize the results of the full-scale test to which the node iterations endured a whole storage time within a silage environment. Within this research, the required capacity was even overestimated to ensure a safety buffer, as NiMh batteries are known to have high discharge rates. Therefore, for satisfactory practical usage, the actual sensor node iterations need a high quantity of batteries in order to work properly for 365 days (RTR nodes = 6 batteries for sensors and additional 6 batteries for the RTR-500 datalogger = 12 batteries in total; LoRa node = 8 batteries in total).

In addition to the required space, the recharging process is a detailed operation. A possibility to reduce the number of batteries could be a charging function during the actual silage storage time. To avoid harming the foil, wireless charging methods as shown by [55] could be used. However, this diminishes the advantages of cost efficiency. A slimming of the nodes' hardware seems to be more appropriate to lower the energy demands. When considering the testing results, it becomes obvious that air pressure sensors can be taken out of consideration in future nodes. Furthermore, Pt100 sensors that need 12 V power should be replaced by sensors which work at 3.3 to 5 V, such as DS18B20, to minimize needed space, cost, and power consumption in particular. Within a laboratory test, we evaluated a modified version of the LoRa node with the above-mentioned changes and a modified timer module. The power consumption of the whole node decreased to 8021 mAh in total at 3.7 V. This consumption can be fed by only two 3.7 V, 4500 mAh batteries. As the sensor node has the capacity for at least three batteries in the spike, a security buffer is supplied, which may also be necessary if the security of the delivered data is increased in future generations. Prodanovic et al. [31] show that in their experimental setup with usage of standard LoRa, e.g., only an authentication of a node within a network consumed up to 7% more energy compared to no authentication. Although an Over The Air Authentication (OTAA) was already used within this research, an additional security buffer for an unusual threat or loss of capacity during storage time would be advantageous and achievable with a third battery.

5.2.2. Data Transmission

High data resilience is assigned for the trials with the RTR module as every sensor is equipped with a dedicated transmission unit. Some RTR modules, however, had transmission issues, even when a gateway was used a few meters away to gain data manually. This can lead back to signal shielding by the module material itself, which consisted of V2A steel. In the development process, these transmission units were replaced by LoRa microcontroller boards.

Treiber et al. [38] compare different transmission technologies. Due to this comparison, it can be pointed out that especially LoRa, based on 868 MHz in Europe, fulfills the need for an automated silage control tool. Furthermore, [39] states that, due to the open-source network, a freedom of scale is given, so that silages can be equipped with dozens of the presented sensors without the need for monthly fees. With a data rate of 0.3 up to 50 kbit/s, a range of up to 10 km, and a high penetration rate through objects, silos can be observed even at distant locations from the farm. It can therefore be assumed that LoRa is able to penetrate "the three different types of obstacles that can be generally

encountered when deploying WSN" [36], which include trees or mobile items, wireless-absorbing or interfering obstacles such as buildings and walls, and a line of sight without any obstacles [36]. Nevertheless, to ensure these aspects, the authors of [36] advise that it is crucial to conduct direct field tests with newly applied ideas, which is taken care of by the large-scale test. The lower the frequency, the higher the capability of penetration through such materials as biomass [56]. With the conception of this module, in comparison to those by [15] and [18], it is not directly necessary to penetrate biomass with a signal, as the head of this trial module is even with the silage surface. There are few, if not zero, centimeters of biomass between the line of sight to the LoRa gateway. The problem of low transmission rates is negligible in these cases as the data packages only consist of the sensor values and are therefore very small. However, the RSSI, pending between −80 and −100, can be classified as weak [57,58]. The antennas in this example were standard dipole Arduino GSM Antenna for MKR 1300. It is already mentioned within the description of these antennas that metal surfaces nearby may influence its coverage [59]. As the node consists of V2A steel, this can be identified as a potentially weak source of signal strength. If the node housing would be manufactured from plastic, possible influences of the metal body can be eliminated in future designs.

Considering the data transmission rates of the LoRa nodes, the maximum possible amount of delivered data packages is attained in minimal time. At the beginning of the trial, approximately 80% of possible packets are delivered, and in the end (40 weeks after start) around 50% are still delivered. This can be attributed to the fact that the battery voltage is decreasing. A decrease in energy can lead to a decrease in reception strength of a sensor network [60,61]. Referring to Figure 5, in the weeks 20 and 38, a dip in the transferred packets can be observed. This breakage can be seen with all sensors and can be traced back to network issues at the farm. The lower amount of data packages of module 7 results from the limited time of "on" intervals by the hardware timer. Other failures (M10 and M8) resulted out of battery shortage. Its origin can be connected to quality issues of the selected hardware and soldering. A quality check run over the course of a few days for each module before usage can fix these problems. However, the available data are sufficient due to the remaining modules. These results show that energy conservation is of great importance to ensure a long period of silage surveillance.

To avoid a lack of data due to any connectivity errors, a storage unit can be constructed, which sends stored data when a successful connection has been restored. Although the rates' monitored parameters in this research are slow, like in many agricultural WSN [32], 1.7 data packets per hour are sent at the end of the 40-week duration, providing an appropriate monitoring frequency and exceeding the suggested amount of one packet per hour. A consistent transmission of data as requested by [32] for an WSN is assured.

Even though the amounts of data sent by the nodes are low, it has been demonstrated in other research that analysis processes can be executed within the sensor node, and only the processed data are sent for storage or decision support [34]. This approach is not applicable to this situation: depending on the location of each node (e.g., sun-covered by walls or weights of the plastic) as well as due to the very heterogenous properties of a silage (DM, spores, bacteria, temperature when being harvested, bulk density, etc.), for most of the gained parameters, no general thresholds can be calculated for every silage as proposed in former research. This stands with the exception of oxygen, as such values should not deviate far from zero after the aerobic phase. In this use case, all data need to be analyzed on a central system, for instance a computing machine on the farm or intrinsic to a cloud system to evaluate the data from one silage heap in total.

Khalifeh et al. [36] state that a need "to develop new algorithms, protocols, low power modules" and more is still prevalent today. Critical to the sensor node technology presented here, the point of end-to-end security for (meta-) data should be taken into focus with its development, as at the moment, the LoRa modules use a standard Over The Air Activation (OTAA) with a lifetime used identification key. Prodanović et al. [31] state that if this

identification (or "secret") key is stolen, the attacker is able to steal the data that is sent by a sensor node.

5.3. Testing Validation

The sensor data show that it is possible to detect signs of spoilage and air breaches within the silage. The temperature within 40 cm depth can provide adequate information about long-term stability or reheating [62]. From this trial, it can be seen that over time the core temperature is decreasing. Pries and Kayser [62] state that the core temperature of silage should be below 15 °C, or it is otherwise assumed that reheating and thus, spoilage, are occurring. However, it can also be observed that core temperature drops down to 15 °C only after more than 150 days. Thaysen [63] states that it is not expedient to look at the core temperature just once, but to permanently log data to see whether it is fluctuating. The author states that higher temperatures within silos can also be caused by uncooled silage. This permanent observation can be granted with this sensor node.

By monitoring the temperature beneath the surface, it becomes obvious that the sensor values are highly dependent on outside factors such as sun radiation and outside temperature. It is only during low-temperature night conditions, when there is no sun radiation to influence the sensors, that a simple standard deviation issue of the data was present after one air breach. The temperature of one node (M4), located nearly 50 cm from the breach, showed a rise four days after air breach number four.

However, biomass, such as silage in particular, has substantial insulation properties not only against heat [30,62] but also against gas flow, depending on its dry matter content and bulk density [8]. The higher the dry matter content of a silage, the higher the bulk density should be to prevent gas exchange [8] and therefore reheating. With an increase in the DM content of grass silage of 20% (from 20% to 40% DM), a higher bulk density of 70 kg DM/m^3 (from 160 to 230 kg DM/m^3) is recommended. A list of adequate bulk densities concerning its dry matter content can be found in [64]. This indicates that if reheating does not take place adjacent to the sensor, it might not be detected with a temperature sensor, as the heat may remain locally restricted. In that case, when reheating is eventually detected, considerable damage may already have been occurred. Nevertheless, temperature data collected over long-term periods can be used to determine the persistent stability of silages and therefore act as a source for models in which weather forecast dependency provide guidance to the farmer on feed-rates per silo and per week. As this research focused on the technological aspects and proof of general functionality, the bulk density of the used silage was not part of investigation. Its influence on the precision of gathered data must be integrated into future research.

Before any air breach is caused, oxygen curves show an unexpected behavior during the beginning of fermentation: the curve decreases to zero within 6 h. This is slower than the literature describes (30 min, [65]). Afterwards, a slight escalation can be observed. This reaction can be explained by a cross-sensitivity of the oxygen sensors with nitrous gases; although a surge in oxygen content after sealing has not been cited in the literature. However, as already mentioned, during the fermentation phase, nitrous gas formations occur in different concentrations. NO, for example, rose within a test by [24] up to 9.71% within a few hours after ensiling and decreased to 0.12% 42 h after ensiling. A laboratory trial with the used chemical sensors and a test gas (30% NO, 70% N) indicated a deflection of the graph. Other nitrous gases may amplify this effect. As the nitrous gases disappear during the first days, this explains the decrease in the graph after several hours of fermentation. With this information, the used sensor node is not only capable of detecting air breaches or spoilage of silage but can also act as a warning tool for farmers, indicating the formation of highly hazardous nitrous gases and when the area around the silo can be safely re-entered again. The behavior of the oxygen sensors during the air breaches shows that it is possible to detect a disruption of the plastic cover. However, a critical result is that the graphs do not show a constant high level of oxygen during disruption, but rather a diurnal pattern.

It is striking that in some cases, the sensor values of O_2 and CO_2, which are very close to the damage, do not react, while sensors roughly 3 meters away do. A reason can be identified within the silage surface topography. Due to the compaction of the silage, a varied and not-homogenous surface is created (Figure 12). Within this surface, several troughs and hills can be identified. As oxygen diffuses very slowly or not at all within silage [29], modules located behind an elevated area are isolated, while others, laying in troughs, are able to detect oxygen.

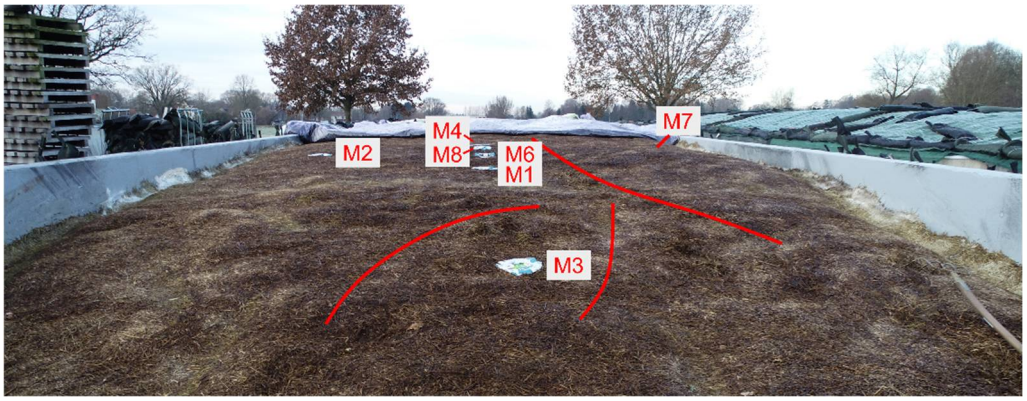

Figure 12. Topography of the full-scale silage test with grass. The surface is not even. It is conceivable that gas flow underneath silage film therefore is influenced by these circumstances.

CO_2 sensors largely show well-defined breakdowns at air breach locations. As the sensors presented very different analog outputs during the field test, these were tested afterwards with calibration gases in a laboratory environment. Although the CO_2 sensors were meant to measure up to 100%, it could be found that the measurement range of used sensors within the trial diverged between 7.9% and 61.6%. This explains why some sensors show a breakdown of CO_2 concentration when the total concentration of CO_2 has reached their measuring capacity. It becomes obvious that in some nodes, oxygen shows no differences while CO_2 curves do so. Well-calibrated carbon dioxide sensors are therefore more capable of detecting air breaches when complemented to oxygen measurements. The literature shows that carbon dioxide and nitrogen share a strong negative correlation within a silo environment [24,28]. The authors state that due to air ingress, a high concentration of nitrogen inflows displaces CO_2. In line, the decrease in CO_2 in the present experiment can be explained by air ingress (due to breaches or air encounters at the silage wall) influencing the correlation between nitrogen and carbon dioxide. It also shows that the measurements of [66], where concentrations of 20–40% within the upper layers of silage can be shown, are snapshots and a comprehensive range can only be detected when permanent CO_2 measurement takes place. This curve has advantages for the farmer. Not only can air breaches be detected, but the overall permeability of a silo can be assessed. When compared over several years, recommendations can be made on how a silo must be managed to maintain a maximum efficiency of sealing (e.g., sealing the walls, etc.).

Humidity levels rise during the trial, and H_2O is formed by fermentation due to nitrous gases [24]. However, the rise in humidity is gradual within this test. Former tests disclosed show faster increases in humidity. This may be justified by the dry matter content of the silage, which is about 50.3%. This content is far too high and should normally be around 30% [10]. In the context of detecting air breaches or spoilage, humidity could be capable of showing changes, but often any detectable changes of the curves lie within 2% or maximum 5% of the values. Therefore, a more accurate absolute sensor should be used, which brings up the question of how often it must be changed within a sensor node, as sensors age and accuracy decreases. Furthermore, additional peaks could be detected which have no relation to the breaches. Respectively, future research should focus on

exploring possible interrelationships between humidity and other factors, implementing humidity as an indicator as well.

Air pressure was examined as well but did not show any deviations from the outside pressure. The sealing conditions are not dense enough to use this as an indicator.

Within the full-scale silage test, it was evident that the sensor node successfully operates under specific circumstances, and it can disclose critical states beneath the plastic cover. TRL 5 (component critical function verification in a relevant environment) [42] has been reached. In order to minimize the number of necessary nodes within a WSN as requested by, e.g., [32], further research has to be conducted with different silage types and varying properties to find the optimal distribution of the nodes in a silage stack.

In general, especially for O_2, a threshold for future integration of an alarm system can be assumed. The rapidly following oxygen content increase after the aerobe phase in silage must be evidence of unusual behavior. Regarding CO_2, it became visible that breakages of more than 5% from the actual concentration are observed when air enters the stack. However, it becomes obvious that over the entire storage period, the CO_2 concentration is decreasing. This decrease can be traced back to reports of air ingress in the literature [24,28]; both the ingress and course of CO_2 are dependent on several unavoidable factors such as silage wall (porosity), plastic cover, or feed out. Therefore, no one unique course can be forecasted for a silage. However, the decrease in CO_2 takes place inertially. To suggest an alarm system working on CO_2 concentration, the mean value for the last 6 h should be compared with the actual sensor value. If this mean value differs by more than 5% of points from the actual value, an air breach can be assumed.

Overall, the used sensors show practicability for the use case. The requirements defined in Section 3.2.1. for each sensor are appropriate. However, the calibration of used sensors needs to be inspected well before their usage as standard calibration "as is" varied greatly by purchased sensors.

6. Conclusions

Within this research, the TRL 5 and the first elements of TRL 6 are realized. Results show that a sensor node capable of detecting negative impacts on silos could be designed and general requirements can be met. Special attention must be given for sensor durability against the oxidative silage environment. In terms of precision, it can be stated that CO_2 does not need a high-precision accuracy readout. For this sensor, a wide measurement range (0–100%) is necessary, and accuracy of $\pm$5% as used in this research is satisfactory, as breakages in CO_2 are normally at least 5% when a leakage in silage appears. As the oxygen content should stay close to 0% when a plastic cover is applied, precise negligible amounts are not critical to report. When considering the parameters of an alarm system, it is only necessary to detect any amount of oxygen higher than 1%. Humidity yielded no reliable results as any anomalies were in the range of measurement errors of the sensor. Nevertheless, humidity at surface levels should be considered in future research. Thus, high accuracy (<1%) is needed. Air pressure is not a necessary factor for sensing any harmful changes. Temperature measurements need to show a high accuracy to sense any changes in an early stage. As reheating due to an oxygen breach appears in a delayed manner, it is not a sufficient as an individual parameter, despite such use in previous research. Nevertheless, as silage quality is dependent on these parameters, an outlook on long-term stability can be constructed, providing farmers with weather-dependent recommended feed rates.

Data transmission via LoRa standard is adequate and, combined with low-power sensors, provides a node battery lifetime of approximately 365 days. As the actual sensor nodes require many batteries, hardware design must be adjusted: an air pressure sensor is not necessary and can be left out; temperature sensors need to be replaced by low-voltage sensors. With such an adapted hardware and a modified timer circuit, required battery capacity as well as node volume can be decreased. Data packet amounts are higher than one packet per hour, even at the end of long-term trials. This data volume transfer rate can be granted as effective.

The conceptualized sensor node shows its capability to protect hardware components against the silage environment. Nevertheless, it should be noted that the choice of the module material impacts on temperature measurements if it is consisting of metals. Additionally, data transmission can be influenced by the usage of such material. Therefore, a plastic-fabricated module is recommended. Sensors must be placed as close to the silage surface as possible for optimal performance.

The module was effectively implemented in a relevant environment. In future research, a provision for the redesign of this node with plastic and exposed sensors should be made. High amounts of data could train artificial intelligence to recognize small deviations or patterns in the data as potential threats. Additionally, with an extensive dataset over different silage types and qualities, along with laboratory-measured silage losses over storage periods, models may be created to not only prevent silage losses, but to also calculate the actual losses due to measured changes in the silage environment. Furthermore, the collected data can contribute to the determination and optimization of the required node number per silage.

Author Contributions: Conceptualization and methodology, J.J.B. and H.B.; writing—original draft preparation, J.J.B.; writing—review and editing, H.S. and H.B.; visualization, J.J.B.; supervision and project administration, H.B.; All authors have read and agreed to the published version of the manuscript.

Funding: Parts of this research were funded by Zill GmbH & Co. KG.

Data Availability Statement: Restrictions apply to the availability of these data. The raw data are not publicly available, as they were collected as part of third-party research.

Conflicts of Interest: The authors declare no conflict of interest.

References

1. Wilkinson, J.M.; Muck, R.E. Ensiling in 2050: Some challenges and opportunities. *Grass Forage Sci.* **2019**, *74*, 178–187. [CrossRef]
2. Wilkinson, J.M.; Lee, M.R.F. Review: Use of human-edible animal feeds by ruminant livestock. *Animal* **2018**, *12*, 1735–1743. [CrossRef] [PubMed]
3. Sucu, E.; Kalkan, H.; Canbolat, O.; Filya, I. Effects of ensiling density on nutritive value of maize and sorghum silages. *Rev. Bras. Zootec.* **2016**, *45*, 596–603. [CrossRef]
4. Dunière, L.; Sindou, J.; Chaucheyras-Durand, F.; Chevallier, I.; Thévenot-Sergentet, D. Silage processing and strategies to prevent persistence of undesirable microorganisms. *Anim. Feed Sci. Technol.* **2013**, *182*, 1–15. [CrossRef]
5. Van den Pol-van Dasselaar, A.; Hennessy, D.; Isselstein, J. Grazing of Dairy Cows in Europe—An In-Depth Analysis Based on the Perception of Grassland Experts. *Sustainability* **2020**, *12*, 1098. [CrossRef]
6. Borreani, G.; Tabacco, E.; Schmidt, R.J.; Holmes, B.J.; Muck, R.E. Silage review: Factors affecting dry matter and quality losses in silages. *J. Dairy Sci.* **2018**, *101*, 3952–3979. [CrossRef] [PubMed]
7. Nußbaum, H. Folienlose Abdeckung von NaWaRo-Silagen: Auswirkungen auf die Silagequalität. In *Effiziente Nutzung von Grünland als Ressource für Die Milch- und Fleischproduktion: 52. Jahrestagung der AGGF vom 28. bis 30. August 2008 in Zollikofen*; Thomet, P., Menzi, H., Isselstein, J., Eds.; Schweizerische Hochschule für Landwirtschaft: Zollikofen, Switzerland, 2008; pp. 238–241, ISBN 978-3-033-01702-3.
8. Thaysen, J. Dichte Controlling- Bedeutung und Instrumente. In *9. Jahrestagung WGM*; Futterkamp, 17–18 August 2008; Wissenschaftliche Gesellschaft der Milcherzeugerberater e.V.: Berlin, Germany, 2008.
9. Köhler, B.; Taube, F.; Ostertag, J.; Thurner, S.; Kluß, C.; Spiekers, H. Dry-matter losses and changes in nutrient concentrations in grass and maize silages stored in bunker silos. *Grass Forage Sci.* **2019**, *74*, 274–283. [CrossRef]
10. Spiekers, H.; Nußbaum, H.; Potthast, V. *Erfolgreiche Milchviehfütterung*, 5th ed.; DLG-Verlag GmbH: Frankfurt am Main, Germany, 2009; ISBN 9783769007305.
11. Spiekers, H. Siliersicherheit. In *Praxishandbuch Futter-und Substratkonservierung*, 8th ed.; DLG-Verlag GmbH: Frankfurt am Main, Germany, 2011; pp. 179–185, ISBN 9783769007916.
12. Jilg, A. Checkliste-Silo-Controlling. Available online: https://docplayer.org/188396104-Checkliste-silo-controlling.html (accessed on 6 September 2019).
13. Wilkins, R.; Wilkinson, M. *Major Contributions in 45 Years of International Silage Conferences*; ISFQC: Piracicaba, Brazil, 2015.
14. Zehetmeier, M.; Läpple, D.; Hoffmann, H.; Zerhusen, B.; Strobl, M.; Meyer-Aurich, A.; Kapfer, M. Is there a joint lever? Identifying and ranking factors that determine GHG emissions and profitability on dairy farms in Bavaria, Germany. *Agric. Syst.* **2020**, *184*, 102897. [CrossRef]

15. Green, O.; Nadimi, E.S.; Blanes-Vidal, V.; Jørgensen, R.N.; Storm, I.M.D.; Sørensen, C.G. Monitoring and modeling temperature variations inside silage stacks using novel wireless sensor networks. *Comput. Electron. Agric.* **2009**, *69*, 149–157. [CrossRef]
16. Williams, A.G.; Hoxey, R.P.; Lowe, J.F. Changes in temperature and silo gas composition during ensiling, storage and feeding-out grass silage. *Grass Forage Sci.* **1997**, *52*, 176–189. [CrossRef]
17. Bochtis, D.D.; Sorensen, C.G.; Green, O.; Bartzanas, T. A diagnostic system for improving biomass quality based on a sensor network. *Sensors* **2011**, *11*, 4990–5004. [CrossRef] [PubMed]
18. Thünen, T.; Heuer, K.; Rochlitzer, R.; Brockmann, C.; Seifert, S. *Effizienzsteigerung im Silageprozess (EiS)—Neue Konzepte zur Minimierung von Energieverlusten*; Julius Kühn-Institut, Federal Research Centre for Cultivated Plants: Quedlinburg, Germany, 2019.
19. Elferink, S.; Driehuis, F.; Gottschal, J.; Spoelstra, S.F. Silage fermentation processes and their manipulation. In *Silage Making in the Tropics with Particular Emphasis on Smallholders, Proceedings of the FAO Electronic Conference on Tropical Silage, 1 September–15 December 1999*; Food and Agriculture Organization of the United Nations: Rome, Italy, 2000.
20. McAllister, T.; Hristov, A. The Funadamentals of Making Good Quality Silage. *Adv. Dairy Technol.* **2000**, *12*, 381–399.
21. Pahlow, G.; Hünting, K. Gärungsbiologische Grundlagen und biochemische Prozesse der Silagebereitung. In *Praxishandbuch Futter- und Substratkonservierung: [Jetzt auch mit Silagen für Biogasanlagen]*, 8th ed.; DLG, Ed.; DLG-Verlag GmbH: Frankfurt am Main, Germany, 2011; pp. 73–82, ISBN 9783769007916.
22. Grothmann, A. Einfluss von Automatischen Fütterungsverfahren in der Milchviehhaltung auf das Tierverhalten und die Futterqualität. Ph.D. Thesis, University of Hohenheim, Hohenheim, Germany, 2015.
23. Rooke, J.A.; Hatfield, R.D. Biochemistry of Ensiling. In *Silage Science and Technology*; Buxton, D.R., Muck, R.E., Harrison, J.H., Eds.; American Society of Agronomy: Madison, WI, USA, 2003; pp. 95–139, ISBN 9780891182344.
24. Wang, L.C.; Burris, R.H. Toxic Gases in Silage, Mass Spectrometric Study of Nitrogenous Gases Produced by Silage. *J. Agric. Food Chem.* **1960**, *8*, 239–242. [CrossRef]
25. Spoelstra, S.F. Nitrate in silage. *Grass Forage Sci.* **1985**, *40*, 1–11. [CrossRef]
26. Kaiser, E.; Weißbach, F. Abbauprodukte des Nitrats bei der Grünfuttersilierung: Ammoniak. In *Berichte der HUB*; Humboldt-Universität zu Berlin: Berlin, Germany, 1988; pp. 29–38.
27. Jilg, A. Bildung von Gärgasen bei der Silagebereitung. Available online: https://www.landwirtschaft-bw.info/site/pbs-bw-new/get/documents/MLR.LEL/PB5Documents/lazbw_gl/Futterkonservierung/G%C3%A4rgase.pdf?attachment=true (accessed on 19 June 2017).
28. Ashbell, G.; Lisker, N. Aerobic deterioration in maize silage stored in a bunker silo under farm conditions in a subtropical climate. *J. Sci. Food Agric.* **1988**, *45*, 307–315. [CrossRef]
29. Rees, D.; Audsley, E.; Neale, M.A. Apparatus for obtaining an undisturbed core of silage and for measuring the porosity and gas diffusion in the sample. *J. Agric. Eng. Res.* **1983**, *28*, 107–114. [CrossRef]
30. Borreani, G.; Tabacco, E. The relationship of silage temperature with the microbiological status of the face of corn silage bunkers. *J. Dairy Sci.* **2010**, *93*, 2620–2629. [CrossRef]
31. Prodanović, R.; Rančić, D.; Vulić, I.; Zorić, N.; Bogićević, D.; Ostojić, G.; Sarang, S.; Stankovski, S. Wireless Sensor Network in Agriculture: Model of Cyber Security. *Sensors* **2020**, *20*, 6747. [CrossRef]
32. García, L.; Parra, L.; Jimenez, J.M.; Parra, M.; Lloret, J.; Mauri, P.V.; Lorenz, P. Deployment Strategies of Soil Monitoring WSN for Precision Agriculture Irrigation Scheduling in Rural Areas. *Sensors* **2021**, *21*, 1693. [CrossRef]
33. Shi, X.; An, X.; Zhao, Q.; Liu, H.; Xia, L.; Sun, X.; Guo, Y. State-of-the-Art Internet of Things in Protected Agriculture. *Sensors* **2019**, *19*, 1833. [CrossRef]
34. Rosero-Montalvo, P.D.; Erazo-Chamorro, V.C.; López-Batista, V.F.; Moreno-García, M.N.; Peluffo-Ordóñez, D.H. Environment Monitoring of Rose Crops Greenhouse Based on Autonomous Vehicles with a WSN and Data Analysis. *Sensors* **2020**, *20*, 5905. [CrossRef] [PubMed]
35. Salleh, A.; Ismail, M.K.; Mohamad, N.R.; Abd Aziz, M.A.; Othman, M.A.; Misran, M.H. Development of Greenhouse Monitoring using Wireless Sensor Network through ZigBee Technology. *Int. J. Eng. Sci. Invent.* **2013**, *2*, 6–12.
36. Khalifeh, A.; Darabkh, K.A.; Khasawneh, A.M.; Alqaisieh, I.; Salameh, M.; AlAbdala, A.; Alrubaye, S.; Alassaf, A.; Al-HajAli, S.; Al-Wardat, R.; et al. Wireless Sensor Networks for Smart Cities: Network Design, Implementation and Performance Evaluation. *Electronics* **2021**, *10*, 218. [CrossRef]
37. Froiz-Míguez, I.; Lopez-Iturri, P.; Fraga-Lamas, P.; Celaya-Echarri, M.; Blanco-Novoa, Ó.; Azpilicueta, L.; Falcone, F.; Fernández-Caramés, T.M. Design, Implementation, and Empirical Validation of an IoT Smart Irrigation System for Fog Computing Applications Based on LoRa and LoRaWAN Sensor Nodes. *Sensors* **2020**, *20*, 6865. [CrossRef] [PubMed]
38. Treiber, M.; Höhendinger, M.; Rupp, H.; Bauerdick, J.J.; Hijazi, O.; Bernhardt, H. Data Transmission and Management for Wireless Sensor Networks in German Dairy Farming Environments. In Proceedings of the XXXVIII CIOSTA & CIGR V International Conference, Rhodes, Greece, 24–26 June 2019.
39. Croce, S.; Tondini, S. Urban microclimate monitoring and modelling through an open-source distributed network of wireless low-cost sensors and numerical simulations. In Proceedings of the 7th International Electronic Conference on Sensors and Applications, online, 15–30 November 2020; MDPI: Basel, Switzerland, 2020; p. 8270.
40. Meligy, R.; Lopez Iturri, P.; Astrain, J.J.; Picallo, I.; Klaina, H.; Rady, M.; Paredes, F.; Montagnino, F.; Alejos, A.; Falcone, F. Low-Cost Cloud Enabled Wireless Monitoring System for Linear Fresnel Solar Plants. In Proceedings of the 7th International Electronic Conference on Sensors and Applications, online, 15–30 November 2020; MDPI: Basel, Switzerland, 2020; p. 8173.

41. Armstrong, K. Emerging Industrial Applications. In *Carbon Dioxide Utilisation*; Elsevier: Amsterdam, The Netherlands, 2015; pp. 237–251, ISBN 9780444627469.
42. Aerospace Standards Committee. *Space Engineering—Definition of the Technology Readiness Levels (TRLs) and Their Criteria of Assessment (ISO 16290:2013, Modified), German Version EN 16603-11:2019*; DIN EN 16603-11; Beuth Verlag GmbH: Berlin, Germany, 2020.
43. Federal Office for Agriculture and Food. Merkblatt-Technologiereifegrade. Available online: https://www.ble.de/SharedDocs/Downloads/DE/Projektfoerderung/Innovationen/Merkblatt-Technologiereifegrade.pdf?__blob=publicationFile&v=3 (accessed on 3 December 2021).
44. Holmes, B.J.; Muck, R.E. Preventing Silage Storage Losses. Available online: https://fyi.extension.wisc.edu/forage/files/2014/01/prevent-silage-storage7.pdf (accessed on 8 July 2021).
45. Winsen. ME2-O2-Φ20 Electrochemical Oxygen Sensor. Available online: http://www.winsen-sensor.com/d/files/PDF/Electrochemical%20Gas%20Sensor/Electrochemical%20Oxygen/ME2-O2-D20%200-25%25%20Manual%20(ver1.2).pdf (accessed on 6 June 2018).
46. PEWATRON. COZIR Ultra Low Power Carbon Dioxide Sensor. 2016. Available online: https://www.pewatron.com/de/aktuelles/news/artikel/cozir-ultraschwachstrom-kohlendioxid-sensormodul/ (accessed on 7 June 2018).
47. Honeywell International, Inc. *HIH-4000 Series Humidity Sensors*; Honeywell International, Inc.: Charlotte, NC, USA, 2010.
48. Freescale Semiconductor. MPX4115, Integrated Silicon Pressure Sensor Altimeter/Barometer Pressure Sensor On-Chip Signal Conditioned, Temperature Compensated and Calibrated—Data Sheet. Available online: https://www.nxp.com/docs/en/data-sheet/MPX4115.pdf (accessed on 7 August 2018).
49. LoRa Alliance. LoRaWAN: What Is It? Available online: https://lora-alliance.org/wp-content/uploads/2020/11/what-is-lorawan.pdf (accessed on 14 September 2021).
50. The Things Industries. ABP vs. OTAA. Available online: https://www.thethingsindustries.com/docs/devices/abp-vs-otaa/ (accessed on 8 March 2022).
51. Bauerdick, J.; Treiber, M.; Bernhardt, H. Smart farming and digitization of research farms—A holistic concept for science and teaching. In *Bio-Economy and Agri-Production: Concepts and Evidence*; Bochtis, D.D., Achillas, C., Banias, G., Lampridi, M., Eds.; Elsevier/Academic Press: Cambridge, MA, USA, 2020; pp. 267–277, ISBN 9780128197745.
52. Bauerdick, J.J.; Treiber, M.; Höhendinger, M.; Hijazi, O.; Schlereth, N.; Bernhardt, H. Sensorsystems in German dairy Farming—Aspects of hardware design and sustainability. In Proceedings of the ASABE Annual International Meeting, Boston, MA, USA, 7–10 July 2019; American Society of Agricultural and Biological Engineers: St. Joseph, MI, USA, 2019.
53. Reid, W.S.; Turnbull, J.E.; Sabourin, H.M.; Ihnat, M. Silo gas: Production and detection. *Can. Agric. Eng.* **1984**, *26*, 197–208.
54. Schweda, E. *Anorganische Chemie*, 17th ed.; Hirzel: Stuttgart, Germany, 2012, ISBN 9783777621340.
55. Santana Abril, J.; Santana Sosa, G.; Sosa, J.; Bautista, T.; Montiel-Nelson, J.A. A Novel Charging Method for Underwater Batteryless Sensor Node Networks. *Sensors* **2021**, *21*, 557. [CrossRef]
56. Larsen, J.J.; Green, O.; Nadimi, E.S.; Toftegaard, T.S. The effect on wireless sensor communication when deployed in biomass. *Sensors* **2011**, *11*, 8295–8308. [CrossRef]
57. Linnemann, M.; Sommer, A.; Leufkes, R. *Einsatzpotentiale von LoRaWAN in der Energiewirtschaft: Praxisbuch zu Technik, Anwendung und Regulatorischen Randbedingungen*, 1st ed.; Springer Vieweg: Wiesbaden, Germany, 2019; ISBN 978-3-658-26917-3.
58. Lam, K.-H.; Cheung, C.-C.; Lee, W.-C. RSSI-Based LoRa Localization Systems for Large-Scale Indoor and Outdoor Environments. *IEEE Trans. Veh. Technol.* **2019**, *68*, 11778–11791. [CrossRef]
59. Arduino Official Store. Dipole Pentaband Waterproof Antenna. Available online: https://store.arduino.cc/products/dipole-pentaband-waterproof-antenna?pr_prod_strat=copurchase&pr_rec_pid=5487963930775&pr_ref_pid=5517873053847&pr_seq=uniform (accessed on 9 December 2021).
60. Zhou, G.; He, T.; Krishnamurthy, S.; Stankovic, J.A. Models and solutions for radio irregularity in wireless sensor networks. *ACM Trans. Sens. Netw.* **2006**, *2*, 221–262. [CrossRef]
61. Rongbiao, Z.; Jianguang, G.; Fuhuan, C.; Yongxian, S. Influence of Supply Voltage of Node on RSSI-Based Localization Performance and Calibration Technique. In Proceedings of the 2011 International Conference on Informatics, Cybernetics and Computer Engineering (ICCE2011), Melbourne, Australia, 19–20 November 2011; Kacprzyk, J., Jiang, L., Eds.; Springer: Berlin/Heidelberg, Germany, 2012; pp. 409–416, ISBN 978-3-642-25184-9.
62. Pries, M.; Kayser, T. Nacherwärmungen bei Grassilagen Vermeiden. Available online: https://www.landwirtschaftskammer.de/landwirtschaft/tierproduktion/rinderhaltung/fuetterung/archiv/nacherwaermung-grassilage.htm (accessed on 3 November 2017).
63. Thaysen, J. Warme Silage: Was ist jetzt noch zu retten? *Top Agrar*, 1 December 2003; R6–R9.
64. Bavarian State Research Center for Agriculture. Controlling am Silo—Steuerung der Silagequalität und möglicher Verluste. Available online: https://www.lfl.bayern.de/mam/cms07/ite/dateien/31396_messprotokoll_und_orientierungswerte.pdf (accessed on 8 March 2022).
65. Woolford, M.K. The detrimental effects of air on silage. *J. Appl. Bacteriol.* **1990**, *68*, 101–116. [CrossRef] [PubMed]
66. Ashbell, G.; Weinberg, Z.G. Top silage losses in horizontal silos. *Can. Agric. Eng.* **1992**, *34*, 171–175.